RESEARCH ARTICLE

Integrated Geophysical and Geospatial Approaches for Delineating Groundwater Potential Zones in Karachi, Pakistan

Muhammad Jahangir Khan[1*]   **Syeda Rida Fatima Bokhari**[2]   **Umair Bin Nisar**[3]   **Farhad Ali**[1]

1. Department of Earth & Environmental Sciences, Bahria University Karachi Campus, Pakistan
2. The State Key Laboratory of Information Engineering in Surveying, Wuhan University, China
3. Centre for Climate Research and Development, COMSATS University, Islamabad Campus, Islamabad, Pakistan

ABSTRACT

Availability of subsurface fresh water in coastal cities of the world is a growing problem due to sea level intrusion and less seepage. The authors have utilized an integrated data dataset in which conventional geophysical methods were used to collect primary data for the groundwater resources in Karachi and geospatial approaches were used to generate the hydrogeological model. It aimed to investigate geological/hydrogeological conditions of any aquifer system in the study area. The geophysical survey was planned to acquire electrical resistivity data in the outskirts of Karachi. The geophysical survey was carried out at twenty-one stations by adopting vertical electrical sounding technique with schlumberger configuration. The field data were processed in an iterative process to improve the signal to noise ratio and obtain smooth field data curves for delineation of the aquifer. The authors have interpreted field data to model the geological information and determine the hydrogeophysical parameters of respective layers. These parameters including the number of layers, aquifer resistivity, aquifer lithology, aquifer thickness and depth to the aquifer, are determined at each field station. The acquired dataset of hydrogeophysical parameters was used to build a geospatial database. The multi-criteria analysis and decision-making process were utilized in GIS-based program to model spatial distribution of these parameters. The results identified an aquifer system in the depth ranging from 53.3 meters to 143.9 meters. The aquifer in the area is mostly sandstone having sufficient thickness which varies from northeast to south and southwest due to undulating topography of the area. The maximum potential of the groundwater is identified in the south which is suitable for water exploration because of low resistivity zone, high aquifer thickness, and flow of drainage network.

*Corresponding Author:
Muhammad Jahangir Khan,
Department of Earth & Environmental Sciences, Bahria University Karachi Campus, Pakistan;
Email: mjahangir.bukc@bahria.edu.pk

1. Introduction

The massive body of sea is at door-step of the coastal towns around the globe. Therefore, the groundwater resources are under threat of advancing saltwater intrusion. Where to drill a borehole for pumping groundwater in a coastal city? It is a challenging and complicated question for town developers, planners, and common public living in coastal regions around the world [1,2]. Centuries ago, people used "dowsing method" [3]. Geophysical and geospatial studies attempt to help in demarcation of the groundwater potential zones to fulfill growing needs of water supply. The geophysical techniques such as electrical resistivity, induced polarization, and electromagnetic induction methods are employed for shallow geological mapping and hydrogeological studies around the globe. These shallow geophysical methods are found helpful within anisotropic medium and to solve water related problems such as exploration for promising aquifer, water pollution monitoring, water management and environmental preservation [4-6]. Hydrogeophysical delineations facilitate obtaining information about aquifer, although sometimes uncertainty in interpretation precludes the recommendation for drilling [7]. The primary difficulties in groundwater modelling can be abridged by interpretation and careful inversion techniques applied to process the resistivity datasets [8,9]. The development of digital data modeling and computer solutions has improved the reliability of geophysical data interpretation [10,11]. Literature review suggests that ground resistivity is a function of various factors which are lithology type of geological layer, mineralogical content and fluid saturation, depth to the geological layer, porosity, and permeability of clastic rocks [12]. The geological environment and recharge potential in an area also affect the resistivity values therefore time series/seasonal analysis of aquifer potential could help to improve the hydrogeological investigations.

Geographical information system (GIS) facilitates in mapping and modelling of spatial databases. For example, the hydrogeophysical database consists of parameters obtained from the geophysical data interpretation [13-15]. GIS-based mapping techniques are effectively used for spatial analysis and decision making. Review of the studies [12,16] suggests that the scope of groundwater studies is broadened by undertaking spatial modelling techniques. GIS-based suitability model for well-location can be created by considering multiple data variables such as layer thickness, depth to aquifer, and ground resistivity of aquifer [17-20].

The coastal cities of Pakistan including Karachi, Thatta, Ormara, Pasni, Gwadar, and other small towns are facing a serious problem in searching of groundwater aquifers. Geoscientists are making their efforts to explore and protect groundwater resources in coastal towns [21-23]. Karachi is one of the largest cities of Pakistan which is further expending in northeastern outskirts. The fast-growing urbanization projects demand mapping of sweet-water aquifers in and around Karachi. Seasonal rainfall is the main source of groundwater recharge in Karachi and its immediate surroundings. Overall, arid climate in the region prevails which limit the recharge potential and channel flow down the streams to southwest. It is speculated that the precipitation rate in Karachi has decreased from 200 mm/yr to 20 mm/yr, majorly causing shifting of monsoon seasonal trends of rain fall system in Karachi region [24,25]. Thereby imbalance between the pumping rate and recharging rate of aquifers imposes adverse impact on quality of groundwater [11]. The present study is designed to investigate hydro-geological conditions of aquifers in hilly outskirts of Karachi city. The objectives are to find the hydrogeological conditions of the subsurface and possible aquifer systems using electrical resistivity method and to classify the region based on spatial analysis of the aquifer and to demarcate the best potential zone to get optimum groundwater.

There are several under-developed towns in northeastern edge of Karachi city. Understudy area is located inside DHA City Karachi (DCK) which is under-development town located to the northeast of Karachi along the motorway section of M-9 (Figure 1a). Khadeji anticline exposed clastic rocks composed of sandstone, shale and limestone in the study area. Hydrological model indicates that the DCK is located in the upper Malir basin, therein two small ephemeral streams known as Abdar and Sukkun and two larger intermittent streams known as Khadeji and Mol are located to the south and north of DCK respectively. These streams drain in Malir river which eventually leads to drain in the Arabian sea (Figure 1b).
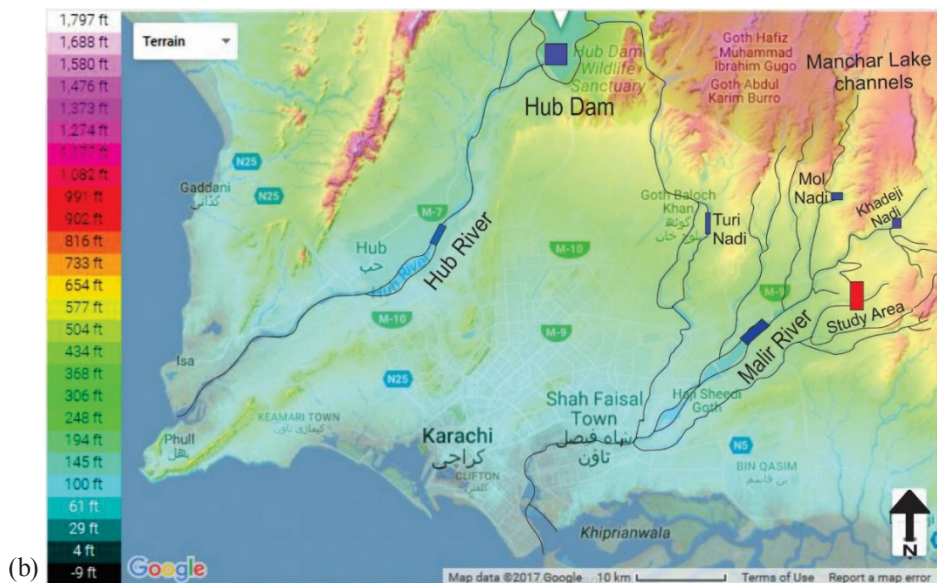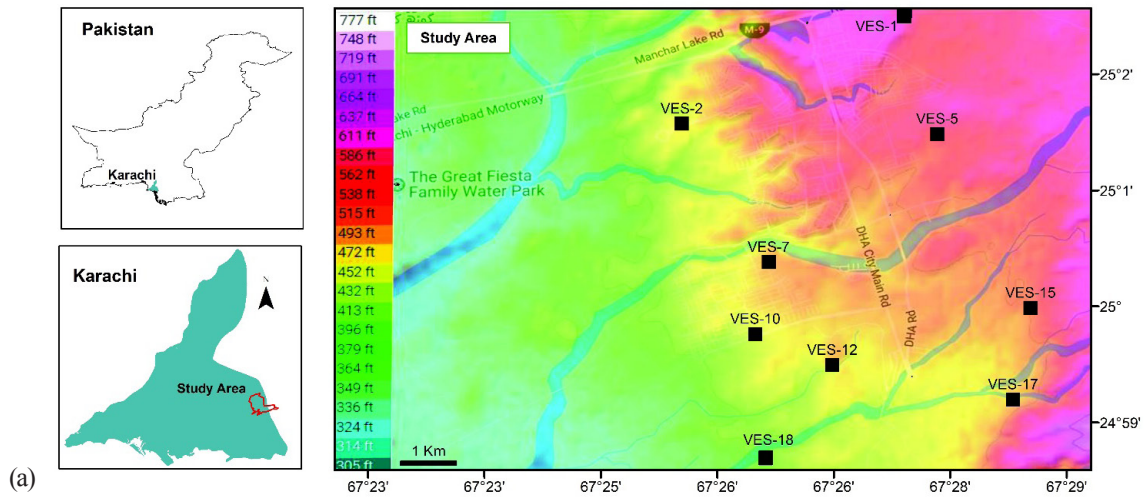
Figure 1. (a). Location of study area and locations of VES points. (b). Hydrological and topographic features in outskirts of Karachi.

2. Data and Methodology

This study is based on acquisition of geophysical dataset using electrical resistivity method, interpretation of field datasets to obtain the hydrogeophysical parameters, and preparation of spatial database for GIS-based modelling.

2.1 Geophysical Data

Geoelectrical resistivity experiments are based on-field measurement of ground resistivity by vertical electrical sounding (VES) [26,27]. The electrodes are configured in co-linear assemblies such as symmetrical Schlumberger and Wenner arrays or asymmetric Dipole-Dipole array. Direct Current supply is compelled to flow in the subsurface, the geological layers resist smooth flow of current,

thus offering ground resistance for each observation. The apparent resistivity is obtained by multiplying ground resistance and geometrical factor (function of distance between the electrodes) at corresponding observation station.

The geophysical field data as VES was acquired at twenty-one stations located in the study area using Schlumberger configuration. The VES stations are spatially distributed over uneven topography of terrain (elevation varies between 430-690 ft above mean sea level). Four electrodes are connected with Terrameter. The potential difference (delta V) was determined between the potential electrodes in response to the direct current supply (I) injected into the ground through current electrodes. These two parameters are used to derive the ground resistance

using Ohm's law. The apparent resistivity (rho-a, also known as ground resistivity) is determined by multiplying the measured resistance and geometric constant at each observation point, as given in Equation (1).

$$\rho_a = \pi \left[\frac{\left(\frac{AB}{2}\right)^2 - \left(\frac{MN}{2}\right)^2}{MN} \right] \frac{\Delta V}{I} \tag{1}$$

where, the current electrode and potential electrode separations are denoted by (AB/2) and (MN/2), respectively.

The apparent resistivity curves (field data curve) are drawn through IPIWIN software. The curves show the apparent resistivity versus current electrode separation along VES profile. The shape of the field curve as H-type, A-type, K-type and Q-type may represent different subterranean conditions [26]. The field data curves are matched with master curves in semi-automation process. The exercise of curve matching attempts to choose a geological model at best-fit match. The best model (with the least error) of the field and master curves helped to infer the characteristics of different geological layers at each VES station. The interpretation based on apparent resistivity provided thickness of each layer, lithology type, (sandstone, shale, Limestone), the thickness of the aquifer etc. The interpretation of VES curves helped us to model the subsurface geology based on resistivity ranges. The hydrogeological conditions such as salinity of groundwater increase when resistivity decreases. A community water well lies near the study area providing a ground control while interpretation of the lithologies down to 450 feet depth. The lithological units encountered in the community borehole are undertaken as benchmark to infer the lithological interpretation of VES curves modelling. The community borehole is producing sweet water from the sandstone as aquifer. The field visit and site observations

suggest that the groundwater is being pumped from a confined aquifer "possible sandstone" with initial smell which indicate the water is not being charged by surface stream or tributary channel. The aquifer lithology is interpreted as sandstone at all VES stations based on contrasting resistivity measurements. The interpretation of VES curves is summarized in geoelectrical sections (graphically represent stratified geological layers). This graphical illustration of geo-electric profile is outlined by layered strata identified through electrical (resistivity) verses depth which are analogous to virtual drilling logs. Thus, the geo-electrical investigations are non-destructive drilling where each layer is discriminated by corresponding apparent resistivity.

The location of VES points (center of Schlumberger array), outer electrode spread (max.), and inferred data for each VES station are summarized in Table 1. The values of apparent resistivity for aquifer (at each VES) are ranging between 101 ohm-m and 269.5 ohm-m (Table 1).

2.2 Geospatial Data

The interpreted hydrogeophysical parameters for each VES station are processed and mapped by the using ArcMap, The interpreted hydrogeophysical variables (location of VES measurements, depth to the aquifer, aquifer resistivity, the yield of the aquifer, and thickness of aquifer) are interpolated by Kriging method. The Kriging method is helpful to generate thematic raster layers of each variable. Each cell of the raster thematic layer is reclassified and multiplied by an assigned weight. The weight of each hydrogeophysical parameters is determined as knowing its proportional influence on the suitability function. The reclassified thematic layers are integrated to

Table 1. The dataset used for mapping of aquifer extent and building the GIS-based suitability criteria.

VES ID	Latitude	Longitude	Max. VES spread (m)	Aquifer resistivity (ohm-m)	Thickness (m)	Yield (gpm)	Aquifer depth (m)	Interpreted lithologies & proposed aquifer (underlilned)
VES-1	25.042398	67.460177	300	115	49.5	155	106	Sh, LSt, Sh, Sh, **S.St,** S.St.
VES-2	25.026230	67.428244	300	101	22.7	70	54.3	Sh, Sh, Sh, **S.St,** Sh, Sh
VES-5	25.024761	67.464804	300	148	50.3	190	79.4	Sh,S.St, Sh, Sh, Sh, **S.St,** Sh
VES-7	25.006357	67.440705	300	138	50.1	210	82.3	S.St, Sh, Sh, **S.St,** Sh, Sh
VES-10	24.996018	67.438758	300	181	36.5	170	53.3	Sh, Sh, Sh, Sh, **S.St**
VES-12	24.991582	67.449782	300	122	60.5	225	94.6	LSt, LSt, Sh, **S.St,** Sh
VES-15	24.999768	67.478147	300	153	36.7	160	73.6	S.St, Sh, **S.St,** Sh, Sh
VES-17	24.986628	67.475659	300	153	65.1	190	76.2	LSt, LSt, Sh, **S.St,** Sh
VES-18	24.967666	67.455622	300	269.5	84.25	250	143.9	Sh, Sh, Sh, **S.St**, LSt

identify the most suitable area (Equation (2)):

$$S_i = \Sigma\, W_i \cdot X_i \qquad (2)$$

W_i = weight of factor map and X_i = criteria class score of factor map "i" and S_i = Suitability index for each pixel in the cell.

The weighted suitability analysis is done by using parametric overlay techniques [2]. For the site suitability analysis, the final map is derived by the following Equation (3):

$$S = (AE_w\, AE_R + AR_W\, AR_R + AZ_W\, AZ_R + AG_W\, AG_R) \qquad (3)$$

where, S is dimensionless, representing site for new well location, AE is the aquifer depth, AR is the aquifer resistivity, AG is aquifer yield, AZ is the aquifer thickness. The subscript letter w represents the weight of each factor and R is the range of each class.

3. Results and Discussion

A correlation between interpreted results at corresponding VES stations such as VES 7, VES 8, VES 9 shows that the presence of aquifer does not extend to the east (Figure 2a). A correlation between interpreted geological layers at VES 10, 12, 17, 16 (from east to west) shows the presence of aquifer (sandstone) (Figure 2b). The sandstone (aquifer) is present at the bottom of lithology log down to 36.5-meter thick package overlain by shale bed at VES-10. In VES-12 the sandstone (aquifer) is present at the bottom of lithology log down to 60-meter thick. The same geological model extends at VES-17, sandstone aquifer is present at the bottom of the lithology log. The correlation shows thick aquifer bottom of the logs (Figure 2b). However, the interpreted aquifer at VES-16 is confined, capped by shale and limited by the underlain limestone.

The correlation of derived lithology log between VES 10, 12, 15 from east to west (Figure 2c). In VES-10 sandstone (aquifer) is present at the bottom up to 36.5-meter thick and shale is present on the top of the geoelectrical section. In VES-12 sandstone (aquifer) is also present at the bottom of lithology log it is very thick package up to 60-meter thick above aquifer shale and limestone is present. In VES-15 we identified two sandstone aquifers bifurcated by the shale bed. The aquifer present at VES-15 is confined aquifer and on the top of lithology log an unconfined aquifer is present. Figure 2d shows a co-relation between VES (1, 5, 8, 18) from North to South, which shows how aquifer is increasing towards South. In VES-1 Sandstone (aquifer) is present at the bottom of lithology log up to 105-meter, and there is a thin package present at the top of the geoelectrical section in VES-1 shale present in between limestone and sandstone (aquifer). Towards south at VES-5 two packages of aquifer are present, one is present at the top and the other one is present at the bottom of the top sandstone (aquifer) which is about 6-meter

thick and at the bottom it is 50.3-meter-thick and shale is present in between these layers. Aquifer thickness is increasing towards south, where there is another very thick aquifer present at the bottom of VES-18 which is about 84 meters thick. This aquifer layer is one of the thickest aquifer of the study area, identified in between VES 5 and VES 18. An unconfined aquifer is present at the top of VES-5.

ArcMap tools are explored to facilitate in optimum site selection for locating potential water zones. which is interpolated to determine lateral extension of aquifer (Figure 3a). The interpolated maps of apparent resistivity are reclassified into five classes. The class one is indicating least suitable area (lowest resistivity), and class at rank five is assigned to the most suitable area (relatively highest resistivity of sandstone aquifer). The most suitable area surrounds VES-18 (which contain the aquifer with the highest resistivity) whereas the least suitable sites are VES-2 and VES-1 (Figure 3b). The field visits to the study area give evidence that the ground water extracted from the study area is being pumped from a confined aquifer characterized with an initial smell.

The depth to the aquifer map showcases the top of aquifer ranging from 53 meters to 143 meters (Figure 3c). The least depth is interpreted at VES-2, 15 & 10, and the deepest aquifer is present at VES-18 (Table 1). Figure 3d represents the reclassified map of aquifer depth into five classes. The value of class one is assigned to the least suitable area (deepest depth aquifer) and the most suitable site is ranked at five (shallowest aquifer) in the southern side of the study area at VES-18. The aquifer thickness map is presenting the interpolated thickness ranging from 29 meters to 77 meters (Figure 3e). The aquifer with the highest thickness is present at VES-18 and least thick is present at VES-2, though these points also contain less depth resistivity and yield values. Figure 3f shows that the class one of the least suitable area (least depth) and five indicates the most suitable (highest depth).

The aquifer yield (gallons per minute) is monitored from the pumping wells installed in the study area. The approximate location of pumping wells is correlated with the VES stations. The interpolated map of values ranging from 93 gpm to 237 gpm, which helps to know the spatial distribution of potential volume and flow dynamics of groundwater in the study area (Figure 3g). The highest yield is present at VES-12 & 18 whereas the least yield is encountered at VES-2. The reclassified map of yield classifies the area into five classes (Figure 3h). The most suitable area is classified as five and least suitable is classified as class one.

Primarily, the hydrogeological information (aquifer yield) and geophysical data (thickness, resistivity, depth)
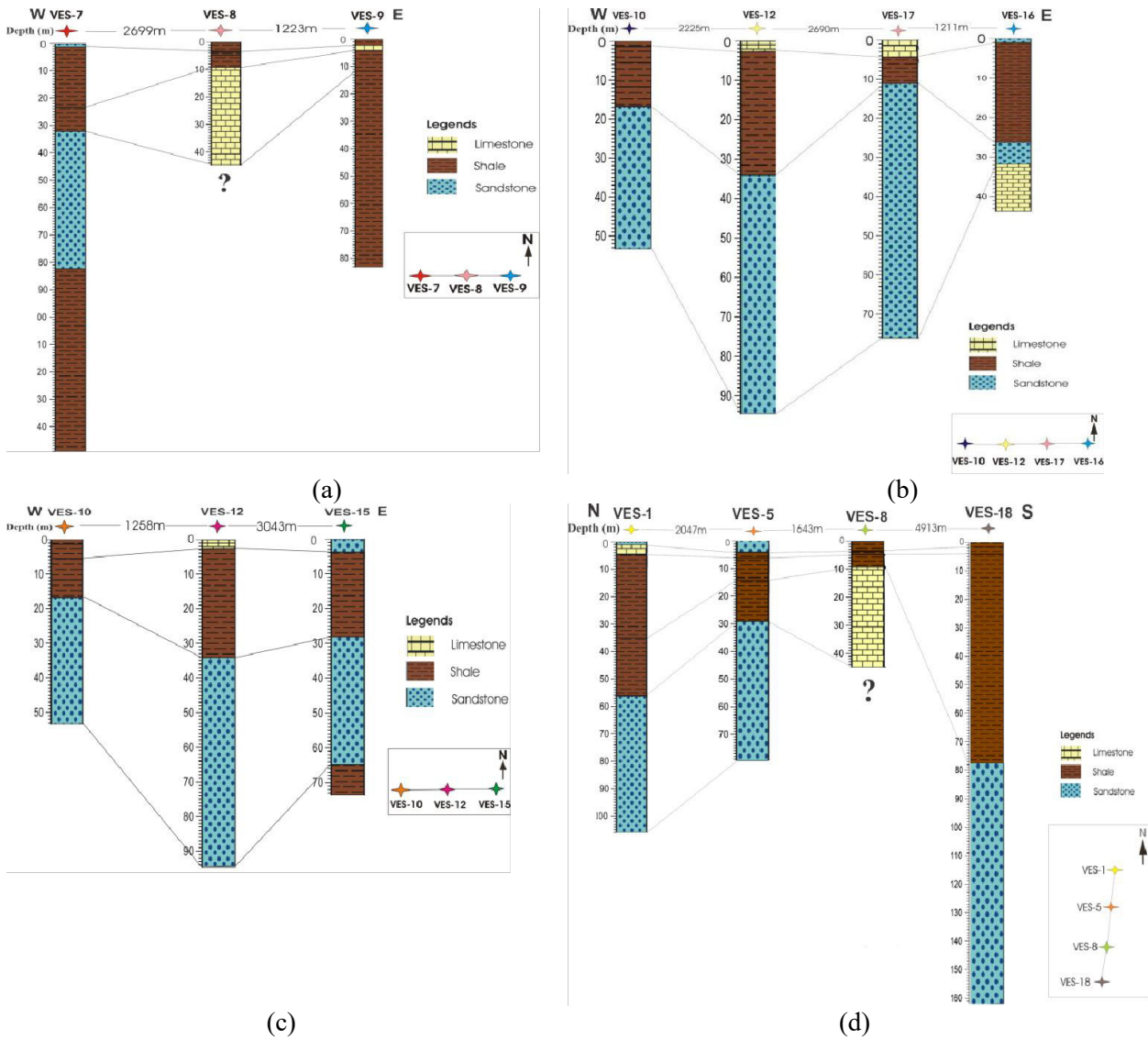
(a)

(b)

(c)

(d)

Figure 2. Geoelectrical sections presenting the interpreted lithologies and their geological correlations.

of the aquifer are used to identify the groundwater potential sites using the geospatial technique. The resultant map is prepared by defining the weight of variables. The aquifer yield is given the highest weight (40%) as an indicative of the aquifer pumping potential, the aquifer nature is represented by the resistivity, though assigned a weight of 30% as an indicator of quality of water either (fresh or saline), resistivity decreases with increases salinity of water, the thickness of the aquifer assigned a weight of 20%, however, relatively least weight i.e. 10% is assigned to the depth of aquifer because it is vital to determine cost of drilling any well. The suitable sites are mapped by weighted overlay method by assigning weight to respective variables such as aquifer yield (40%), aquifer resistivity (30%), aquifer thickness (20%), and aquifer depth (10%). The suitability analysis is done through overlay analysis of the spatially distributed variables (Figure 3).

Site suitability analysis depends on inputs variables of hydrogeophysical database, which were interpolated, reclassified, and integrated for weighted overlay analysis. The integration of the data is shown in the suitability map. The map classifies the study area into three classes (Figure 4). The suitability map showcases potential groundwater zones in the study area and provides a guide to select a site for installation of a water-well. Each pixel of the integrated raster indicates its suitability value. For instance, the pixel with a value of 3 is the most suitable area (shown in green). The similar pixel values are grouped to showcase the lateral extent of most suitable zone. The observation sites are overlaid to recognize the location of the VES point and intended drilling. The most suitable area contains multiple wells in the buffer of VES-18, 12, 17, 10, 7
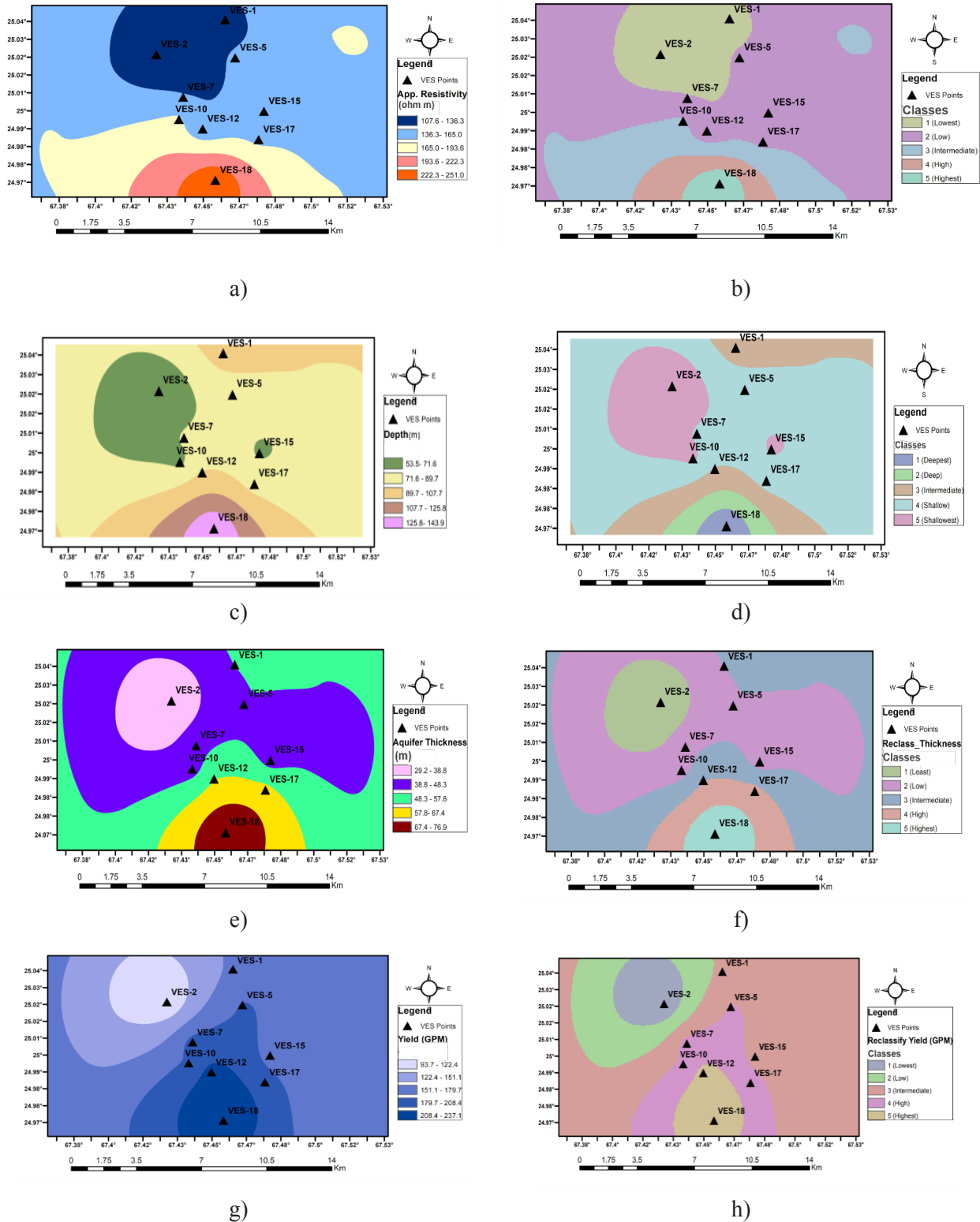
Figure 3. GIS-based maps of input variables of suitability criteria. a) Aquifer Apparent Resistivity map, b) Reclassified Apparent Resistivity map, c) Aquifer Depth map, d) Reclassified Aquifer Depth map, e) Aquifer thickness map, f) Reclassified Aquifer thickness map, g) Aquifer yield (GPM) map, h) Reclassified Aquifer yield (GPM) map.
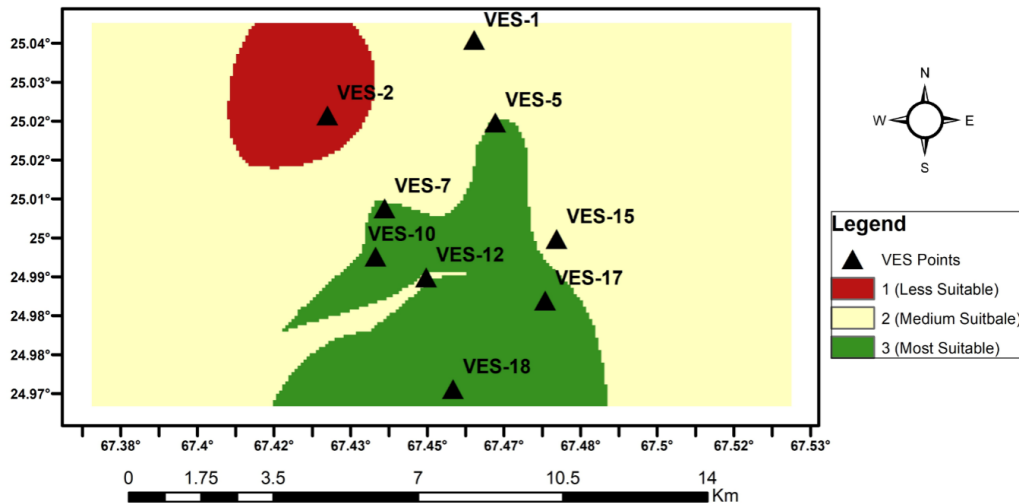
Figure 4. Groundwater potential zonation. Site suitability map is classifying the study area for locating a new well.

and 5. The least suitable area is in the vicinity of VES-2, which may be not good for drilling a water well.

4. Conclusions

The geophysical delineations of VES helped to explore the hydrogeological conditions of the aquifer in study area. It is found that the electrical resistivity methods are significant to find the aquifer characteristics. The sandstone layer was interpreted as an aquifer however, its thickness varies in its lateral extent within in hilly topography of study area. The integrated approaches of geophysical and GIS helped to integrate the multiple parameters and classify the region into potential zones. The suitable sites of potential groundwater are located in vicinity of VES 18, 12, 17, 10, 7, 5 (central-south) of the study area. The most suitable potential zone is recommended for drilling water well in the future. This study may help in cutting down the cost of water exploration projects and reduces the labor efforts in hunting possible sites for drilling a well. The integrated methodological approach of this study is recommended to utilize for locating groundwater potential zones even in rough and hilly regions.

Author Contributions

Muhammad Jahangir Khan has initiated this research work's proposal and designed the methodological workflow. Syeda Rida Fatima Bokhari and Farhad Ali assisted in the literature review, data analysis and interpretation. Umair Bin Nisar helped in the improvement of the language while proofreading of article. All authors have read and agreed to the published version of the manuscript.

Funding

Acknowledgments

Data Availability Statement

The data presented in this study are available on request from the corresponding author. Data is contained within the article.

Conflict of Interest

The authors declare no conflict of interest.

References

[1] Li, P., Zhang, C., Li, W., et al., 2021. Groundwater vulnerability assessment of Pingtan Island in Fuzhou City, China, based on DRASLI-QUE. Journal of Hydrologic Engineering. 26(3), 05020050.

[2] Motevalli, A., Pourghasemi, H.R., Hashemi, H., et al., 2019. Assessing the vulnerability of groundwater to salinization using GIS-Based data-mining techniques in a coastal aquifer. Spatial modeling in GIS and R for earth and environmental sciences. Elsevier: Amsterdam. pp. 547-571.

[3] Pérez-Carrascal, K., García-Guarín, J., 2021. Detection of water leaks with Dowsing technique and

Reynold's transport theorem. Journal of Physics: Conference Series. IOP Publishing. (1), 012004.

[4] Mondal, N.C., Singh, V.P., Singh, V.S., et al., 2010. Determining the interaction between groundwater and saline water through groundwater major ions chemistry. Journal of Hydrology. 388(1-2), 100-111.

[5] Prasad, K.A., Gnanappazham, L., Selvam, V., et al., 2015. Developing a spectral library of mangrove species of Indian east coast using field spectroscopy. Geocarto International. 30(5), 580-599.

[6] Greer, B.M., Burbey, T.J., Zipper, C.E., et al., 2017. Electrical resistivity imaging of hydrologic flow through surface coal mine valley fills with comparison to other landforms. Hydrological Processes. 31(12), 2244-2260.

[7] Thabit, J.M., AL-Hameedawie, M.M., 2014. Delineation of groundwater aquifers using VES and 2D imaging techniques in north Badra area, Eastern Iraq. Iraqi Journal of Science. 55(1), 174-183.

[8] Kearey, P., Brooks, M., 1991. An introduction to geophysical prospecting. Blackwell: Boston.

[9] Teixidó, T., 2012. The surface geophysical methods: A useful tool for the engineer. Procedia Engineering. 46, 89-96.

[10] Stewart, M.T., 1982. Evaluation of electromagnetic methods for rapid mapping of salt-water interfaces in coastal aquifers. Groundwater. 20(5), 538-545.

[11] Khan, M.J., Shah, B., Nasir, B., 2020. GIS-based groundwater quality assessment for drinking purpose: A case study of Sindh industrial trading estate (SITE), Karachi, Pakistan. Modelling Earth Systems and Environment. 6, 263-272.

[12] Al-Ruzouq, R., Shanableh, A., Merabtene, T., et al., 2019. Potential groundwater zone mapping based on geo-hydrological considerations and multi-criteria spatial analysis: North UAE. Catena. 173, 511-524.

[13] Yin, L., Zhang, E., Wang, X., et al., 2013. A GIS-based DRASTIC model for assessing groundwater vulnerability in the Ordos Plateau, China. Environmental Earth Sciences. 69(1), 171-185.

[14] Dashtpagerdi, M.M.,Vagharfard, H., Honarbakhsh, A., et al., 2013. GIS-based fuzzy logic approach for identification of groundwater artificial recharge site. Open Journal of Geology. 3(06), 379.

[15] Ghorbanzadeh, O., Feizizadeh, B., Blaschke, T., 2018. Multi-criteria risk evaluation by integrating an analytical network process approach into GIS-based sensitivity and uncertainty analyses. Geomatics, Natural Hazards and Risk. 9(1), 127-151.

[16] Biswas, S., Mukhopadhyay, B.P., Bera, A., 2020. Delineating groundwater potential zones of agriculture dominated landscapes using GIS based AHP techniques: A case study from Uttar Dinajpur district, West Bengal. Environmental Earth Sciences. 79(12), 1-25.

[17] Metwaly, M., El-Qady, G., Massoud, U., et al., 2010. Integrated geoelectrical survey for groundwater and shallow subsurface evaluation: A case study at Siliyin spring, El-Fayoum, Egypt. International Journal of Earth Sciences. 99(6), 1427-1436.

[18] Khan, S., Nisar, U., Ehsan, S., et al., 2021. Aquifer vulnerability and groundwater quality around Brahma Bahtar Lesser Himalayas Pakistan. Environmental Earth Sciences. 80(13), 1-13.

[19] Nisar, U., Khan, M.J., Imran, M., et al., 2021. Groundwater investigations in the hattar industrial estate and its vicinity, Haripur District, Pakistan: An integrated approach. Kuwait Journal of Science. 48(1), 51-61.

[20] Aziz, N.A., Hasan, R.H., Abdulrazzaq, Z.T., 2018. Optimum site selection for groundwater wells using integration between GIS and hydrogeophysical data. Engineering and Technology Journal. 36(6 Part (A) Engineering), 596-602.

[21] Abdalla, O.A., Ali, M., Al-Higgi, K., et al., 2010. Rate of seawater intrusion estimated by geophysical methods in an arid area: Al Khabourah, Oman. Hydrogeology Journal. 18(6), 1437-1445.

[22] Olusola, F.O., Marvellous, O.O., 2020. Groundwater vulnerability mapping and quality assessment around coastal environment of Ilaje local government area, southwestern Nigeria. International Journal of Earth Sciences Knowledge and Applications. 2(2), 74-91.

[23] Khan, M.J., Zeeshan, M., Ali, S.S., 2020. GIS-based change detection of coastal features along Karachi Coast, Pakistan. Pakistan Journal of Science. 72(2), 124-133.

[24] Zafar, S., Zaidi, A., 2019. Impact of urbanization on basin hydrology: A case study of the Malir Basin, Karachi, Pakistan. Regional Environmental Change. 19(6), 1815-1827.

[25] Salma, S., Shah, M.A., Rehman, S., 2012. Rainfall trends in different climate zones of Pakistan. Pakistan Journal of Meteorology. 9(17).

[26] Xie, J., Cui, Y.A., Fanidi, M., et al., 2021. Numerical modeling of marine self-potential from a seafloor hydrothermal ore deposit. Pure and Applied Geophysics. 178(5), 1731-1744.

[27] Sato, M., Mooney, H.M., 1960. Electrochemical mechanism of sulphide self-potentials. Geophysics. 25, 226-249.